24. T. B. Mitchell, J. J. Bollinger, D. H. E. Dubin, X.-P. Huang, W. M. Itano, in preparation (preprint available at www.boulder.nist.gov/timefreq/ion/penning/pop/pop.pdf).

25. Minimization of the energy was carried out numerically for given areal density by allowing the positions of the planes to vary with respect to one another within the external potential and by varying the lattice structure within the planes. We made the simplifying assumption, which was consistent with the experimental observations, that the lattice structure of each plane was identical. The areal density of the planar OCP is a control parameter that, when varied, leads to transitions in both the number and lattice structure of the planes. This theory focuses on the minimum potential energy states while neglecting finite temperature effects that may be important (particularly effects that are near the continuous phase transitions where large structural fluctuations may occur).

26. T. M. O'Neil and D. H. E. Dubin, *Phys. Plasmas* **5**, 2163 (1998).

27. V. I. Valtchinov, G. Kalman, K. B. Blagoev, *Phys. Rev. E* **56**, 4351 (1997).

28. R. H. Baughman, J. M. Shacklette, A. A. Zakhidov, S. Stafstrom, *Nature* **392**, 362 (1998).

29. R. Lakes, *Science* **235**, 1038 (1987).

30. This manuscript is a work of the U.S. government; it is not subject to U.S. copyright. This research was supported by the Office of Naval Research and NSF (D.H.E.D.). We thank B. King, R. J. Rafac, J. P. Schiffer, and D. J. Wineland for useful comments and B. M. Jelenković and J. N. Tan for technical assistance.

14 August 1998; accepted 14 October 1998

Controlling Factors for the Brittle-to-Ductile Transition in Tungsten Single Crystals

Peter Gumbsch,* Joachim Riedle, Alexander Hartmaier, Hellmut F. Fischmeister

Materials performance in structural applications is often restricted by a transition from ductile response to brittle fracture with decreasing temperature. This transition is currently viewed as being controlled either by dislocation mobility or by the nucleation of dislocations. Fracture experiments on tungsten single crystals reported here provide evidence for the importance of dislocation nucleation for the fracture toughness in the semibrittle regime. However, it is shown that the transition itself, in general, is controlled by dislocation mobility rather than by nucleation.

Some materials are brittle and shatter like glass, whereas others are ductile and deformable. Several materials, such as the refractory metals, steels, and semiconductor crystals, exhibit both types of behavior (*1–5*) with a brittle-to-ductile transition (BDT) at a characteristic temperature. A crack introduced into a material may propagate as a brittle crack with an atomically sharp crack front; alternatively, the material near the crack tip may show sufficient plasticity to slow down or arrest the crack. Crack-tip plasticity comprises two distinct processes, nucleation of dislocations at or near the crack tip and their propagation away from the crack. Several models describe the BDT as a nucleation-controlled event (*6, 7*), and others focus on dislocation mobility as the controlling factor (*8–10*).

The experimental evidence on the controlling factors of the BDT, which has been obtained mostly from silicon single crystals, remains inconclusive. On the one hand, the temperature at which the BDT occurs [BDT temperature (BDTT)] is strongly dependent on the strain rate, which allows an activation energy for the BDT to be determined. This activation energy has been shown to be equal to that for dislocation motion (*2, 8, 9*), which suggests a mobility-controlled BDT. On the other hand, specimen size and the availability of dislocation sources have a pronounced influence on the fracture toughness to the degree that they may even switch the material's behavior from brittle to ductile (*11*).

We performed cleavage experiments on tungsten single crystals to determine the controlling factors of the BDT. To exclude disturbances from grain boundaries, single crystals were chosen. Fracture toughness tests were performed on all four low-index crack systems. A crack system is specified by the nominal crack plane and the crack front direction. The four crack systems studied are therefore denoted as $\{100\}\langle 010\rangle$, $\{100\}\langle 011\rangle$, $\{110\}\langle 1\bar{1}0\rangle$, and $\{110\}\langle 001\rangle$ in crystallographic notation. The temperature range covered by the experiments was between the liquid nitrogen temperature (77 K) and 650 K. The toughness tests were performed on high-purity (*12*) tungsten single crystal bars (3 mm by 6 mm by 30 mm) loaded in three-point bending. To obtain a well-defined value for the fracture toughness, a sharp crack front was introduced by precracking at 77 K. Precrack length was evaluated from the compliance and, where possible, was also determined postmortem on the fracture surfaces, where faint arrest lines are visible. The tests were performed with a constant loading rate, which translates into an almost constant stress intensity rate of 0.10 ± 0.02 MPa $\mathrm{m}^{1/2}$/s (*13*). More details of the experimental procedure are given in (*14*).

Multiple tests (more than five) were conducted for all four crack systems at room temperature and at 77 K. Several individual tests at other temperatures were performed to determine the temperature dependence of the fracture toughness (Fig. 1). Macroscopically, the transition from brittle to ductile response usually correlates with the maximum in fracture toughness. The temperature at this maximum was taken as the BDTT and was determined from Fig. 1 within 30 to 60 K (Table 1). The so-defined BDTTs fell into an interval of 100 K for all four crack systems, even though both $\{110\}$ crack systems had a significantly higher room temperature fracture toughness than the $\{100\}$ systems (Table 1).

Testing at 77 K always resulted in brittle cleavage fracture on the precrack plane for all four crack systems. The load-displacement curves showed perfectly linear behavior up to the load at which fracture occurred. The fracture surfaces were clean except for a few river lines.

At room temperature and above, most of the fracture specimens revealed small deviations from linearity in the load-displacement curves before final fracture, indicating a limited amount of plastic relaxation. The fracture surfaces were significantly rougher than those of the precracks and of the specimens tested at 77 K. Cleavage below the BDTT was always catastrophic. No noticeable amount of slow crack growth was observed.

The preexisting dislocation density and the availability of dislocation sources can be increased by plastic deformation before toughness testing. Specimens with a $\{110\}\langle 1\bar{1}0\rangle$ crack system were deformed by compression along the $\langle 110\rangle$ (long) axis at 400°C to a plastic strain of $\varepsilon_{\mathrm{pl}} = 0.1$ before precracking. At low temperatures the predeformed specimens are significantly tougher than the unde-

Table 1. BDTT and fracture toughness of tungsten single crystals for the {100} and {110} cleavage planes with different crack front directions. Fracture toughness at room temperature K^{RT} and at liquid nitrogen temperature $K^{77\mathrm{K}}$ are mean values from at least five individual measurements (standard deviation in parentheses). Fracture toughness is in MPa $\mathrm{m}^{1/2}$.

Crack system	BDTT (K)	K^{RT}	$K^{77\mathrm{K}}$
$\{100\}\langle 010\rangle$	470	8.7 (2.5)	3.4 (0.6)
$\{100\}\langle 011\rangle$	370	6.2 (1.7)	2.4 (0.4)
$\{110\}\langle 001\rangle$	430	20.2 (5.5)	3.8 (0.4)
$\{110\}\langle 1\bar{1}0\rangle$	370	12.9 (2.1)	2.8 (0.2)

Max-Planck-Institut für Metallforschung, Seestrasse 92, 70174 Stuttgart, Germany.

*To whom correspondence should be addressed. E-mail: gumbsch@finix.mpi-stuttgart.mpg.de

formed specimens (Fig. 2). However, their fracture toughness remains almost constant, increasing only marginally up to 370 K. Above this temperature a drastic increase in fracture toughness is observed. The BDT occurs at about 470 K, which is 100 K higher than in the undeformed material.

At higher temperatures, up to the BDTT, a higher loading rate always lowers the fracture toughness (Fig. 3). At room temperature, the fracture toughness decreases linearly with the logarithm of the loading rate from 16 to 6 MPa $m^{1/2}$ when the loading rate is increased from 0.04 to 6 MPa $m^{1/2}/s$. Furthermore, the BDTT increases significantly with the loading rate. In an Arrhenius plot (log $\dot{K}$ versus 1/BDTT), all values fall on a straight line, yielding an activation energy for the BDT in tungsten of $Q_{BDT} \approx 0.2$ eV.

At low temperatures, in contrast, the results of the mechanical tests reveal a unique value for the fracture toughness of single crystals independent of the loading rate. This value is close to but somewhat larger than the minimal fracture toughness predicted from the surface energy (*15*). The low-temperature fracture toughness shows a dependence on the state of predeformation and the crystallographic orientation of the crack. It varies not only with the cleavage plane but also with the propagation direction within a given cleavage plane. This influence of the propagation direction was analyzed in detail elsewhere and was interpreted as an anisotropy of the lattice trapping (*15, 16*).

The increase of the fracture toughness with temperature in the semibrittle fracture regime below the BDTT is more difficult to interpret. The fracture surfaces of {110} specimens tested at higher temperatures show many more steps and facets than the fracture surfaces from the low-temperature tests. In contrast, the appearance of {100} fracture surfaces does not vary significantly with temperature. In any case, the significant increase in fracture toughness with temperature has to be interpreted as the onset of plastic deformation in the vicinity of the crack tip. The increased dislocation activity causes a blunting of the crack tip. Furthermore, dislocations cause a severe stress relaxation at the crack tip by shielding it from the applied load.

In tungsten, dislocations penetrating the fracture surface can be made visible by chemical etching with an aqueous solution of $K_3Fe(CN)_6$ and NaOH (*17*). This process is highly anisotropic and gives best results on tungsten {100} surfaces, whereas no etch pits are produced on {110} surfaces (*18*). Dislocation etch pits on the {100}<010> fracture surface produced at 77 K reveal the activity of a few discrete dislocation sources at the arrest line of the precrack (Fig. 4A). In contrast, after fracture at room temperature, dislocation etch pits show a very dense population of dislocation sources along the crack front (Fig. 4B). The length of the dislocation traces emanating from these sources, however, is only slightly greater than in the low-temperature fracture.

The topology of the crack front and of the precrack do not vary significantly with the testing temperature, because all specimens were precracked at 77 K. Thus, the increase in the density of dislocation sources at higher testing temperatures suggests that additional sources are activated. A high density of dislocation sources along the crack tip is necessary to produce global shielding of the crack tip, because the zone of effective shielding may be localized around a source (*19*). Only when this global shielding is achieved does the size of the plastic zone, and thus dislocation mobility, become important.

Evidence for the importance of the number of active dislocation sources from our experiments on predeformed samples has been presented. A similar increase in fracture toughness upon predeformation has also been observed in NiAl single crystals (*5*) and in silicon (*20*).

Homogeneous predeformation increases the density of dislocations throughout the material. If the dislocation population around the crack tip were regarded simply as a polarizable medium, one would expect a lower fracture toughness with increased dislocation density (polarizability), because the beneficial shielding dislocations would move away from the crack tip

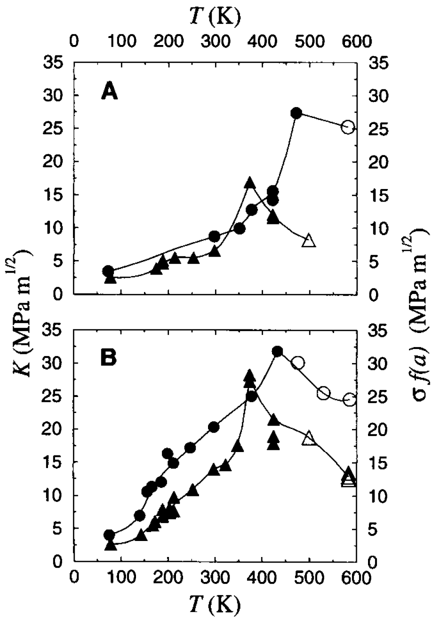

Fig. 1. Dependence of fracture toughness on temperature *T* and crystallographic orientation of the sample. Results for {100} fracture surfaces are displayed in (**A**), and those for {110} fracture surfaces are shown in (**B**). The <001> crack front is indicated by circles and the <011> front is indicated by triangles. Filled symbols represent fracture toughnesses (left axis) and open symbols represent stresses at failure, which are normalized by crack length *a* for compatibility with the fracture toughness scale (right axis). Lines are shown only as a visual guide.

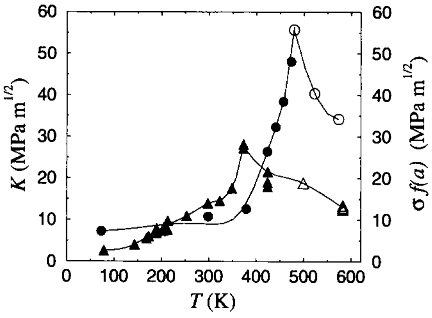

Fig. 2. Temperature dependence of predeformed samples (circles) compared with undeformed reference samples (triangles). Remaining assignments are as in Fig. 1.

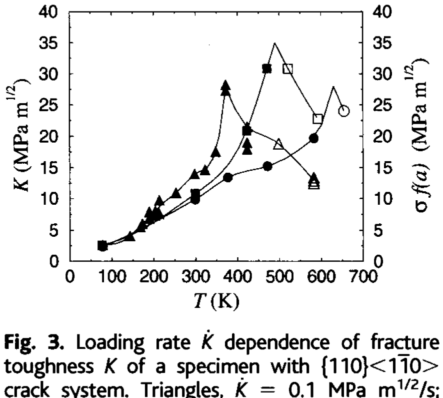

Fig. 3. Loading rate $\dot{K}$ dependence of fracture toughness *K* of a specimen with {110}<1$\bar{1}$0> crack system. Triangles, $\dot{K}$ = 0.1 MPa $m^{1/2}/s$; squares, $\dot{K}$ = 0.4 MPa $m^{1/2}/s$; circles, $\dot{K}$ = 1.0 MPa $m^{1/2}/s$. Remaining assignments are as in Fig. 1.

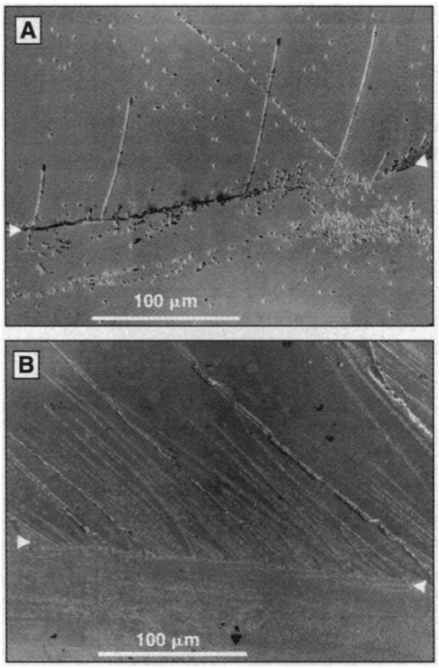

Fig. 4. Fracture surface of a {100}<010> crack produced at 77 K (**A**) and at 298 K (**B**). Arrowheads mark arrest front of the precrack.

and the fracture-promoting dislocations would move closer to the crack tip (*21*). Additional energy dissipation by dislocation motion is insignificant compared with crack-tip shielding at these low temperatures. Low-temperature fracture toughness increases with predeformation; thus other processes must be invoked. The only reasonable explanation is that the preexisting dislocations in the highly stressed vicinity of the crack tip act as sources for dislocations, which provide more efficient shielding.

At intermediate temperatures, the beneficial effect of the predeformation vanishes and the fracture toughness of the predeformed specimens is lower than that of the reference specimens. This is attributed to the increased yield strength and lower dislocation mobility produced by work hardening. The reduced dislocation mobility will not only decrease the fracture toughness but must also be expected to shift the BDTT to higher temperatures. Similar behavior is also found in NiAl single crystals (*5*). These observations strongly indicate that the BDT is controlled by dislocation mobility.

At low temperatures, dislocation nucleation is the limiting process because of the scarcity of active sources. When the temperature is sufficiently high to activate a large number of sources, or the number of active sources is increased by predeformation, dislocation mobility assumes control of the nucleation rate, and the fracture toughness becomes rate dependent. Such a loading rate dependence of the fracture toughness of tungsten is found in room temperature experiments but not at liquid nitrogen temperature. It is evident that any model for the BDT must necessarily include dislocation mobility and cannot be based exclusively on dislocation nucleation.

In the whole temperature regime of the present investigation, plasticity in tungsten is believed to be controlled by the mobility of the screw dislocations [for example, see (*22*)]. However, the activation energy for the glide of these dislocations is $Q_{\mathrm{screw}} = 2$ eV (*23, 24*), whereas the activation energy for the BDT $Q_{\mathrm{BDT}} = 0.2$ eV is much closer to the activation energy for the glide of nonscrew (edge) dislocations, $Q_{\mathrm{edge}} = 0.2$ to 0.5 eV (*23, 25*). Consequently, development of a plastic zone at the crack tip cannot be limited by the same mechanisms as bulk plasticity. A possible mechanism to lower the high activation barrier for screw dislocation motion could involve the high-stress region around the crack tip. If a dislocation—either one that is generated at the crack tip or a preexisting one—moves in the "singular" stress field along the crack tip, it will generate dislocation segments of nonscrew character parallel to the crack tip, which are highly mobile and must be expected to provide highly efficient shielding. However, the detailed mechanisms for the different crystallographic orientations of the crack remain to be clarified.

The results clearly show that the fracture toughness in the semibrittle fracture regime below the BDTT is strongly dependent on the availability and activity of dislocation sources. However, it becomes evident that, in materials other than dislocation-free silicon, the BDT itself is not controlled by the availability of sources but must be interpreted as a thermally activated process controlled by the mobility of dislocations.

References and Notes

1. C. St. John, *Philos. Mag.* **32**, 1193 (1975).
2. M. Brede and P. Haasen, *Acta Metall.* **36**, 2003 (1988).
3. S. G. Roberts, A. S. Booth, P. B. Hirsch, *Mater. Sci. Eng.* **A176**, 91 (1994).
4. H. Huang and W. W. Gerberich, *Acta Metall. Mater.* **42**, 639 (1994).
5. F. Ebrahimi and S. Shrivastava, *Acta Mater.* **46**, 1493 (1998).
6. J. R. Rice and R. Thomson, *Philos. Mag. A* **29**, 73 (1974).
7. M. Khantha, D. Pope, V. Vitek, *Phys. Rev. Lett.* **73**, 684 (1994).
8. P. B. Hirsch, S. G. Roberts, J. Samuels, *Proc. R. Soc. London Ser. A* **421**, 25 (1989).
9. S. G. Roberts, in *Computer Simulations in Materials Science*, series E: *Applied Sciences*, vol. 308, H. O. Kirchner, L. P. Kubin, V. Pontikis, Eds. (Kluwer, Dordrecht, Netherlands, 1996), pp. 409–433.
10. A. Hartmaier and P. Gumbsch, *Phys. Status Solidi B* **202**, R1 (1997).
11. G. Michot, M. A. L. de Oliveira, A. George, *Mater. Sci. Eng.* **A176**, 99 (1994).
12. J. Riedle, P. Gumbsch, H. F. Fischmeister, V. G. Glebovsky, V. N. Semenov, *Mater. Lett.* **20**, 311 (1994).
13. The variability in the stress intensity rate mainly stems from variations in the length of the precrack.
14. J. Riedle, thesis, Universität Stuttgart, Stuttgart (1995).
15. J. Riedle, P. Gumbsch, H. F. Fischmeister, *Phys. Rev. Lett.* **76**, 3594 (1996).
16. S. Kohlhoff, P. Gumbsch, H. F. Fischmeister, *Philos. Mag. A* **64**, 851 (1991).
17. L. Berlec, *J. Appl. Phys.* **33**, 197 (1962).
18. Y. Tamura, T. Fujii, Y. Ohba, *Trans. Inst. Met.* **14(5)**, 173 (1972).
19. B. Devincre and S. G. Roberts, *Acta Mater.* **44**, 2891 (1996).
20. J. Samuels and S. G. Roberts, *Proc. R. Soc. London Ser. A* **421**, 1 (1989).
21. S. J. Zhou and R. Thomson, *J. Mater. Res.* **6**, 1763 (1991).
22. A. S. Argon and S. R. Maloof, *Acta Metall.* **14**, 1449 (1966).
23. U. Ziebart, thesis, Universität Stuttgart, Stuttgart (1986).
24. D. Brunner, personal communication.
25. H. W. Schadler, *Acta Metall.* **12**, 861 (1964).

26. J.R. thanks S. Roberts for helpful discussions and hospitality at the University of Oxford, where part of this work was conducted. J.R. gratefully acknowledges partial financial support from Deutscher Akademischer Austauschdienst. A.H. acknowledges financial support from Deutsche Forschungsgemeinschaft (contract GU 367/1).

22 July 1998; accepted 8 October 1998

A Tough, Thermally Conductive Silicon Carbide Composite with High Strength up to 1600°C in Air

Toshihiro Ishikawa,* Shinji Kajii, Kenji Matsunaga,
Toshihiko Hogami, Yasuhiko Kohtoku, Toshio Nagasawa

A sintered silicon carbide fiber–bonded ceramic, which consists of a highly ordered, close-packed structure of very fine hexagonal columnar fibers with a thin interfacial carbon layer between fibers, was synthesized by hot-pressing plied sheets of an amorphous silicon-aluminum-carbon-oxygen fiber prepared from an organosilicon polymer. The interior of the fiber element was composed of sintered β-silicon carbide crystal without an obvious second phase at the grain boundary and triple points. This material showed high strength (over 600 megapascals in longitudinal direction), fibrous fracture behavior, excellent high-temperature properties (up to 1600°C in air), and high thermal conductivity (even at temperatures over 1000°C).

Silicon carbide fiber–reinforced ceramic matrix composites (SiC-CMCs) are being developed as a candidate for toughened thermostructural materials (*1*). However, at present, no SiC-CMCs can withstand actual long use at high temperatures (>1500°C) in air, because of the problems of heat resistance or oxidation resistance or both of the fiber and interphase (*2, 3*). Moreover, under load, cracks in the matrix caused by creep failure of the fiber also accelerate fatal oxidation of the composites (*4*). We developed a type of toughened SiC-based material containing perfectly close-packed, very fine hexagonal columnar fibers that consist of a sintered structure of β-SiC crystals. At the interface between the hexagonal columnar fibers,

---

Ube Research Laboratory, Corporate Research and Development, Ube Industries Limited, 1978-5 Kogushi, Ube City, Yamaguchi 755, Japan.

*To whom correspondence should be addressed. E-mail: 24613u@ube-ind.co.jp